polymers

MDPI

Article

Design Analysis of Adhesively Bonded Structures

Ee-Hua Wong [1,2,*] and Johan Liu [3,4]

1 Sino-Singapore International Joint Research Institute, Guangzhou 510550, China
2 Energy Research Institute, Nanyang Technological University, Nanyang 639798, Singapore
3 Microtechnology and Nanoscience, Chalmers University of Technology, Se41296 Gothenburg, Sweden; johan.liu@chalmers.se
4 SMIT Center, Shanghai University, No 20, Chengzhong Road, Shanghai 201800, China
* Correspondence: ehwong@ntu.edu.sg; Tel.: +64-22-095-3011

Received: 23 October 2017; Accepted: 27 November 2017; Published: 1 December 2017

Abstract: The existing analytical solutions for the peeling and shearing stresses in polymeric adhesively bonded structures are either too inaccurate or too complex for adoption by practicing engineers. This manuscript presents a closed-form solution that is reasonably accurate yet simple and concise enough to be adopted by practicing engineers for design analysis and exploration. Analysis of these concise solutions have yielded insightful design guidelines: (i) the magnitude of peeling stress is generally higher than that of shearing stress; (ii) the peeling stress in a balanced structure may be reduced most effectively by reducing the elastic modulus of the adherends or by increasing the adhesive-to-adherend thickness ratio and less effectively by reducing the elastic modulus of the adhesive; and (iii) the peeling stress in an unbalanced structure may be reduced by increasing the in-plane compliance of the structure, which may be implemented most effectively by reducing the thicknesses of the adherends and less effectively by reducing the elastic modulus of the adherends.

Keywords: balanced structures; unbalanced structures; single lap joint; closed-form solutions

1. Introduction

The polymeric adhesive in many bonded structures is much more structurally compliant than the adherends, leading to a significantly lower magnitude of in-plane stress in the adhesive. Completely ignoring this in-plane stress in the adhesive substantially reduces the complexity of the analysis and allows the formulation of closed-form solutions. The first of such analyses was presented by Volkersen (1938) [1], who modelled the adhesive layer in a single lap-shear structure as having only shear stiffness and the adherends as capable of only in-plane stretching. A more sophisticated analysis was presented by Goland and Reissner (1944) [2], who modelled the adhesive as having stiffness in shearing and transverse stretching and the adherends as capable of in-plane stretching and bending.

Goland and Reissner [2] assumed the adherends to have negligible shear and transverse-normal compliances, which may not be valid for bonded structures with relatively large ratios of adherends-to-adhesive thicknesses. Assuming a linear distribution of shear stress along the thickness of the adherends—An overly simplistic assumption—Tsai et al. (1998) [3] incorporated shear compliance of the adherends into the formulation of Goland and Reissner [2]. But before Tsai et al. [3], Suhir (1986, 1989) has evaluated the shear compliance [4] and the transverse compliance [5] of the adherends using Ribiere Solution for a long-and-narrow strip [6].

Besides assuming nil in-plane stress in the adhesive, the above authors and many others [7–12] have also conveniently assumed that the shear and the transverse stresses are unvarying over the thickness of the adhesive. Ojalo and Eidinoff (1978) [13] were believed to be the first to challenge this assumption; assuming linear variation of the in-plane and the transverse deformations of the adhesive along its thickness, they concluded that the shear stress varies linearly while the transverse stress is

unvarying along the thickness of the adhesive. More recently, Wang and Zhang (2009) [14] assumed that transverse stress in the adhesive exhibits a step-jump in magnitude while shear stress is unvarying along its thickness. These assumptions invariably violate the differential equation of equilibrium:

$$\begin{aligned} \frac{\partial \sigma_x}{\partial x} + \frac{\partial \tau_{xz}}{\partial z} &= 0 \\ \frac{\partial \sigma_z}{\partial z} + \frac{\partial \tau_{xz}}{\partial x} &= 0 \end{aligned} \tag{1}$$

Except for [14], these strength-of-material solutions have also failed to satisfy the condition that there shall be no shear stress at the free edges of the adhesive, thus leading to gross underestimation of the magnitude of peeling stress at the free edge [15].

Moreover, the strength-of-material solution of Goland and Reissner [2] was restricted to balanced structures—That is, structures in which the adherends are identical in geometry and materials—For which the resultant differential equations for the shear and the transverse stresses in the adhesive are uncoupled and can be solved with relative ease. Delale et al. (1981) [8], Bigwood and Crocombe (1989) [9], Liu et al. (2014) [11], Zhao et al. (2011) [16], and Zhang et al. (2015) [17] have analysed unbalanced structures experiencing arbitrary edge loading such that the differential equations are heavily coupled. The resultant closed-formed solutions are immensely chunky and complex.

A "theory of elasticity" solution that is based on variational formulation was presented by Allman (1977) [18]. The solution satisfied Equation (1) while also ensuring that the free-edge condition of nil-shear stress was satisfied. Similar approach was followed by Chen and Cheng (1983) [19], Yin (1991) [20], Adams and Mallick (1992) [21], and Wu and Zhao (2013) [22]. The solutions are not only complex but highly restrictive—The boundary conditions are embedded within the governing differential equation, thus limiting the generality of the solutions.

From the perspective of practicing engineers, the current state of closed-form solutions for adhesively bonded structures is far from satisfactory—These solutions are either too inaccurate or too complex for practical adoption. It is the objective of this manuscript to offer a closed-form solution that is reasonably accurate yet simple and concise enough to be adopted by practicing engineers for design analysis and exploration.

2. Analytical Equations

Figure 1 shows a bonded structure made up of adherend #1, adherend #2, and adhesive #3. The structure experiences a mismatched thermal expansion between the adherends and stretching, shearing, and bending at their edges. Note the notations and positive directions of the in-plane stretching forces $N_{\pm il}$, the shear forces $Q_{\pm il}$, moments $M_{\pm il}$, and curvatures $\kappa_{\pm il}$, at $x = \pm l$, where l is the half-length of the adhesive. The height, Young's modulus, shear modulus, flexural stiffness, and thermal coefficient of expansion of member #i are denoted as h_i, E_i, G_i, D_i, and α_i, respectively. The shear, in-plane (x), transverse (z), and flexural compliances of the bonded structure are denoted as κ_s, λ_x, λ_z, and $\overline{D}$, respectively. The corresponding compliances of member #i are denoted as κ_{si}, λ_{xi}, λ_{zi}, and $\overline{D_i}$, respectively. The formulas for computing these compliances are collected under the heading "basic formula" at the front of this article. The derivations of these formulas may be found in Refs. [15,23].

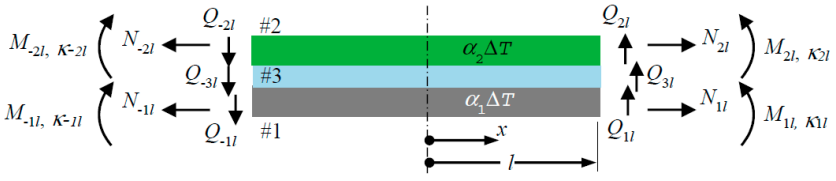

Figure 1. Schematic of a bonded structure experiencing general conditions of edge loading and thermal strain.

The adhesive is assumed to experience negligible in-plane stress, σ_x. The differential equation of equilibrium, Equation (1), then suggests an nonvarying shear stress, τ_{xz}, and a linearly varying transverse stress, σ_z, along the thickness of the adhesive. Denoting σ_m and σ_a respectively as the mean and amplitude of variation of the transverse stress along the thickness of the adhesive, the peeling stress at the two interfaces of the adhesive with adherend #*i* is given by

$$\sigma_{pi} = \sigma_m \mp \sigma_a,\ i = 1, 2 \tag{2}$$

Unless otherwise stated in this manuscript, the upper and the lower signs in $\mp$ are associated with adherend #1 and adherend #2 respectively. These stresses, together with the interfacial shear stress, τ, on an elemental representation of a bonded structure are shown in Figure 2. Substituting $\partial\sigma_z/\partial z$ as $\sigma_a/(2h_3)$ into Equation (1) gives

$$\sigma_a = -\frac{h_3}{2}\frac{d\tau}{dx} \tag{3}$$

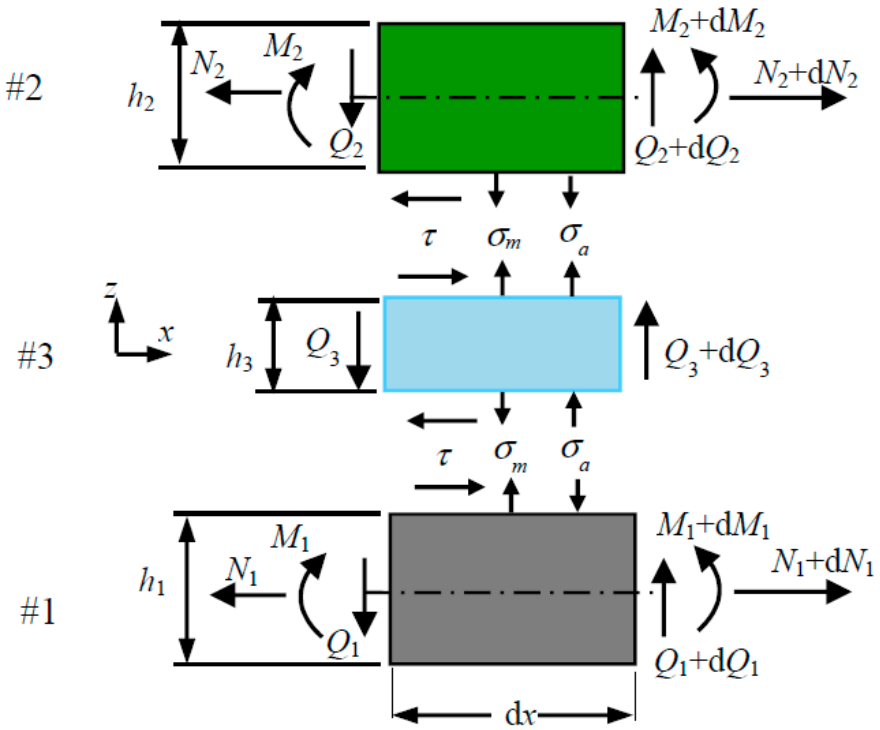

Figure 2. Elemental representation of a bonded structure.

The derivations of the differential equations for τ and σ_m are elaborated upon in Appendix A.

2.1. Balanced Structures

Referring to Equation (A5) and with the parameter, μ_σ, equates to nil for a balanced bonded structure, the differential equation for the interfacial shear stress is given by

$$\frac{d^3\tau}{dx^3} - \beta^2\frac{d\tau}{dx} = 0 \tag{4}$$

where $\beta^2 = \lambda_x/\kappa_s$. For structures of reasonably large length, say $\beta l > 3$, the solution is given approximately by

$$\tau(x) = A_c e^{\beta(x-l)} + A_3,\ x > 0 \tag{5}$$

The boundary conditions $\kappa_s d\tau(l)/dx = \varepsilon_T + \varepsilon_{Nl} + \varepsilon_{Ml}$ and $\int_{-l}^{l} \tau dx = N_{2l} - N_{-2l}$ return

$$\begin{aligned} A_{\pm c} &= \tfrac{\varepsilon_T + \varepsilon_{\pm Nl} + \varepsilon_{\pm Ml}}{\beta \kappa_s} \\ A_3 &= \tfrac{N_{2l} - N_{-2l}}{2l} - \tfrac{A_c - A_{-c}}{2\beta l} = \tfrac{N_{2l} - N_{-2l}}{2l} - \tfrac{\varepsilon_{Nl} - \varepsilon_{-Nl} + \varepsilon_{Ml} - \varepsilon_{-Ml}}{2\lambda_x l} \end{aligned} \tag{6}$$

where

$$\begin{aligned} \varepsilon_T &= (\alpha_2 - \alpha_1)\Delta T \\ \varepsilon_{\pm Nl} &= N_{\pm 2l}\lambda_{x2} - N_{\pm 1l}\lambda_{x1} \\ \varepsilon_{\pm Ml} &= \tfrac{1}{2}((h_1 + h_3)\kappa_{\pm 1l} + (h_2 + h_3)\kappa_{\pm 2l}) \end{aligned} \tag{7}$$

Referring to Equation (A6) and with the parameter, μ_τ, equates to nil for a balanced bonded structure, the differential equation for the mean of the peeling stress is given by

$$\frac{d^4\sigma_m}{dx^4} + 4\alpha^4\sigma_m = 0 \tag{8}$$

where $4\alpha^4 = \overline{D}/\lambda_z$. For structures of reasonably large length, say $\alpha l > 3$, the solution is given approximately by

$$\sigma_m(x) = e^{\alpha(x-l)}[B_{1c}\cos\alpha(x-l) + B_{2c}\sin\alpha(x-l)],\ x > 0. \tag{9}$$

The boundary conditions $\lambda_z d^2\sigma_m/dx^2 = M_{2l}/D_2 - M_{1l}/D_1 = \hat{M}_{21l}$ and $\lambda_z d^3\sigma_m/dx^3 = -(Q_{2l}/D_2 - Q_{1l}/D_1) = -\hat{Q}_{21l}$ return

$$B_{1c} = \frac{\hat{Q}_{21l}}{2\alpha^3\lambda_z} + B_{2c}, B_{2c} = \frac{\hat{M}_{21l}}{2\alpha^2\lambda_z} \tag{10}$$

Substituting Equation (5) into Equation (3) yields the amplitude of the peeling stress:

$$\sigma_a(x) = -\frac{A_s\beta h_3}{2}e^{\beta(x-l)} \text{ for } x > 0. \tag{11}$$

2.2. Unbalanced Structures

2.2.1. Non-Free Edge Solutions

Combining Equations (A5) and (A6) gives rise to a seventh-order differential equation for $\tau(x)$ and a sixth-order differential equation for $\sigma_m(x)$ [5,7–9,11]. The resulting solutions are far too complex to be attractive to practicing engineers. Instead, solving Equations (A5) and (A6) iteratively would lead to approximate solutions of $\tau(x)$ and $\sigma_m(x)$ that are far simpler, thus enabling insights and encouraging application by practicing engineers. Designating the subscripts c and p as complimentary and particular solutions, respectively, the approximate solution involves solving for the complementary solutions for the interfacial shear stress, τ_c, and the mean of the peeling stress, σ_{mc}—these are given by Equations (5) and (9)—followed by substituting σ_{mc} into Equation (A5) to obtain $\tau = \tau_c + \tau_p$, and τ_c into Equation (A6) to obtain $\sigma_m = \sigma_{mc} + \sigma_{mp}$.

The interfacial shear and peel stresses have been evaluated as

$$\begin{aligned} \tau(x) &= A_s e^{\beta(x-l)} + A_4 + e^{\alpha(x-l)}\left[A_{p1}\cos\alpha(x-l) + A_{p2}\sin\alpha(x-l)\right] \\ \sigma_m(x) &= e^{\alpha(x-l)}[B_1\cos\alpha(x-l) + B_2\sin\alpha(x-l)] + B_p e^{\beta(x-l)} \\ \sigma_a(x) &= -\tfrac{h_3}{2}\left[\beta A_s e^{\beta(x-l)} + \alpha e^{\alpha(x-l)}\left[\left(A_{p1} + A_{p2}\right)\cos\alpha(x-l) - \left(A_{p1} - A_{p2}\right)\sin\alpha(x-l)\right]\right] \end{aligned} \tag{12}$$

where

$$\begin{aligned}
A_s &= A_c - \tfrac{\alpha\left(A_{p1}+A_{p2}\right)}{\beta} \\
A_4 &= A_3 - \tfrac{1}{2l}\left(\tfrac{1}{2\alpha} - \tfrac{\alpha}{\beta^2}\right)\left(A_{p1} - A_{-p1}\right) + \tfrac{1}{2l}\left(\tfrac{1}{2\alpha} + \tfrac{\alpha}{\beta^2}\right)\left(A_{p2} - A_{-p2}\right) \\
A_{\pm p1} &= \tfrac{\mu_\sigma}{\kappa_s}\tfrac{\left(2\alpha^3+\alpha\beta^2\right)B_{\pm 1c}+\left(2\alpha^3-\alpha\beta^2\right)B_{\pm 2c}}{2\alpha^2\left(4\alpha^4+\beta^4\right)},\ A_{p2} = \tfrac{\mu_\sigma}{\kappa_s}\tfrac{\left(2\alpha^3+\alpha\beta^2\right)B_{\pm 2c}-\left(2\alpha^3-\alpha\beta^2\right)B_{\pm 1c}}{2\alpha^2\left(4\alpha^4+\beta^4\right)} \\
B_{\pm 1c} &= \tfrac{\hat{Q}_{\pm 21l}}{2\alpha^3\lambda_z} + B_{\pm 2c}, B_{\pm 2c} = \tfrac{\hat{M}_{\pm 21l}}{2\alpha^2\lambda_z} \\
B_1 &= \tfrac{\beta^3 B_p+\hat{Q}_{21l}/\lambda_z}{2\alpha^3} + B_2, B_2 = \tfrac{-\beta^2 B_P+\hat{M}_{21l}/\lambda_z}{2\alpha^2} \\
B_P &= \tfrac{\mu_\tau A_c}{\lambda_z}\tfrac{\beta}{4\alpha^4+\beta^4}
\end{aligned} \tag{13}$$

It is worth noting that in the case of an unbalanced bonded structure experiencing only mismatched thermal expansion and/or differential stretching between the adherends, the magnitude of σ_m is negligibly small compared to that of τ and σ_a [23]. Ignoring σ_m, the differential equation for τ is given by Equation (4); and $\tau(x)$ and $\sigma_a(x)$ are given by Equations (5) and (11), respectively.

2.2.2. Free Edge Solutions

The expression of shear stress in Equation (12) does not satisfy the free edge condition, $\tau(l) = 0$, which is essential for accurate modelling of $\sigma_a(l)$. The free edge condition may be enforced artificially through the introduction of a decay function, $1 - e^{n\beta(x-l)}$ [15,23]. The derivation of the factor n is explained in Appendix B. The expressions of $\tau(x)$, $\sigma_m(x)$, and $\sigma_a(x)$ with the free edge condition enforced are given by

$$\tau(x) = \left\{A_s e^{\beta(x-l)} + A_4 + e^{\alpha(x-l)}\left[A_{p1}\cos\alpha(x-l) + A_{p2}\sin\alpha(x-l)\right]\right\}\left[1 - e^{n\beta(x-l)}\right] \tag{14}$$

$$\begin{aligned}
\sigma_m(x) &= e^{\alpha(x-l)}\left[B_{1n}\cos\alpha(x-l) + B_{2n}\sin\alpha(x-l)\right] + B_p e^{\beta(x-l)} - B_{pn1}e^{(n+1)\beta(x-l)} - B_{pn2}e^{n\beta(x-l)} \\
&\approx e^{\alpha(x-l)}\left[B_{1n}\cos\alpha(x-l) + B_{2n}\sin\alpha(x-l)\right] + B_p e^{\beta(x-l)}
\end{aligned} \tag{15}$$

$$\sigma_a(x) = -\frac{h_3}{2}\left\{\begin{array}{l}\left(1 - e^{n\beta(x-l)}\right)\left\{\beta A_s e^{\beta(x-l)} + \alpha e^{\alpha(x-l)}\left[\left(A_{p1}+A_{p2}\right)\cos\alpha(x-l) - \left(A_{p1}-A_{p2}\right)\sin\alpha(x-l)\right]\right\} - \\ n\beta e^{n\beta(x-l)}\left\{A_s e^{\beta(x-l)} + A_4 + e^{\alpha(x-l)}\left[A_{p1}\cos\alpha(x-l) + A_{p2}\sin\alpha(x-l)\right]\right\}\end{array}\right\} \tag{16}$$

where

$$\begin{aligned}
B_{1n} &= \tfrac{\beta^3\left(B_p-(n+1)^3 B_{pn1}-n^3 B_{pn2}\right)+\hat{Q}_{21l}/\lambda_z}{2\alpha^3} + B_{2n}, B_{2n} = \tfrac{-\beta^2\left(B_p-(n+1)^2 B_{pn1}-n^2 B_{pn2}\right)+\hat{M}_{21l}/\lambda_z}{2\alpha^2} \\
B_{pn1} &= \tfrac{\mu_\tau A_c}{\lambda_z}\tfrac{(n+1)\beta}{4\alpha^4+(n+1)^4\beta^4}, B_{pn2} = \tfrac{\mu_\tau A_3}{\lambda_z}\tfrac{n\beta}{4\alpha^4+n^4\beta^4}
\end{aligned} \tag{17}$$

3. Numerical Validations

Equations (5), (9), and (11) for the balanced structures [15] and for unbalanced bonded structure experiencing only mismatched thermal expansion and/or differential stretching between the adherends [23] have been validated in previous publications. Hence, only the equations for unbalanced structures experiencing the general state of edge loading shall be validated. The material properties, dimensions of the bonded structure, thermomechanical loads, and finite element model used in this study are shown in Figure 3a. The domain of the bonded structure was modelled using more than 100,000 eight-node quadrilateral elements. The domain around the free edge was discretised at 75 divisions per mm. The adhesive was assigned with anisotropic properties of negligible E_x, rendering it consistent with the assumption in the analytical solutions that the adhesive experiences negligible σ_x. The compliances (assuming plane stress), characteristic parameters (α, β), free-edge parameters (ϕ, n) which are computed using Equations (A9) and (A10), coupling parameters (μ_σ, μ_τ), and the coefficients

in the stress equations are tabulated in Table 1. It is noted that (i) βl, $\alpha l \geq 4$, thus justifying the use of the reduced form of solutions as presented in Section 2; (ii) the magnitudes of the coupling parameters are significantly large, reflecting the significant difference in the stiffness between the two adherends; and (iii) the relatively strong coupling has led to the relatively large magnitudes of the particular stress coefficients (A_{p1}, A_{p2}, B_p) compared to that of the complementary stress coefficients (A_s, B_{1n}, B_{2n}).

Figure 3b shows the shear stress, $\tau(x)$, for (i) the analytical solution that enforces the nil-shear stress free-edge condition, Equation (14), (ii) the analytical solution that does not enforce the above free-edge condition, Equation (12), and (iii) the finite element analysis (FEA) solution. The analytical solution, Equation (14), agrees reasonably well with the FEA solution for the entire length of the bonding although the magnitude of the former is consistently at approximately 85% that of the FEA. The free-edge parameter at $\phi = 0.45$ is in reasonable agreement with that extracted from FEA at $\phi_{FEA} =$ 0.40 and 0.48 for $-l \leq x \leq 0$ and $0 \leq x \leq -l$, respectively.

Figure 3c shows the mean of the transverse stress, $\sigma_m(x)$, for (i) the analytical solution that enforces the nil-shear stress free-edge condition, Equation (15), (ii) the analytical solution that does not enforce the above free-edge condition, Equation (12), and (iii) the FEA solution. The free-edge solution, Equation (15), agrees well with the FEA solution, especially if the FEA solutions at $x = \pm l$, which are susceptible to numerical error, are ignored.

Figure 3d shows the amplitude of the transverse stress, $\sigma_a(x)$, for (i) the analytical solution that enforces the nil-shear stress free-edge condition, Equation (16), (ii) the analytical solution that does not enforce the above free-edge condition, Equation (12), and (iii) the FEA solution. Both Equation (16) and the FEA show the magnitude of σ_a increases rapidly near the free edge. In contrast, Equation (12) shows a very mild increase in magnitude near the free edge, in the opposite direction.

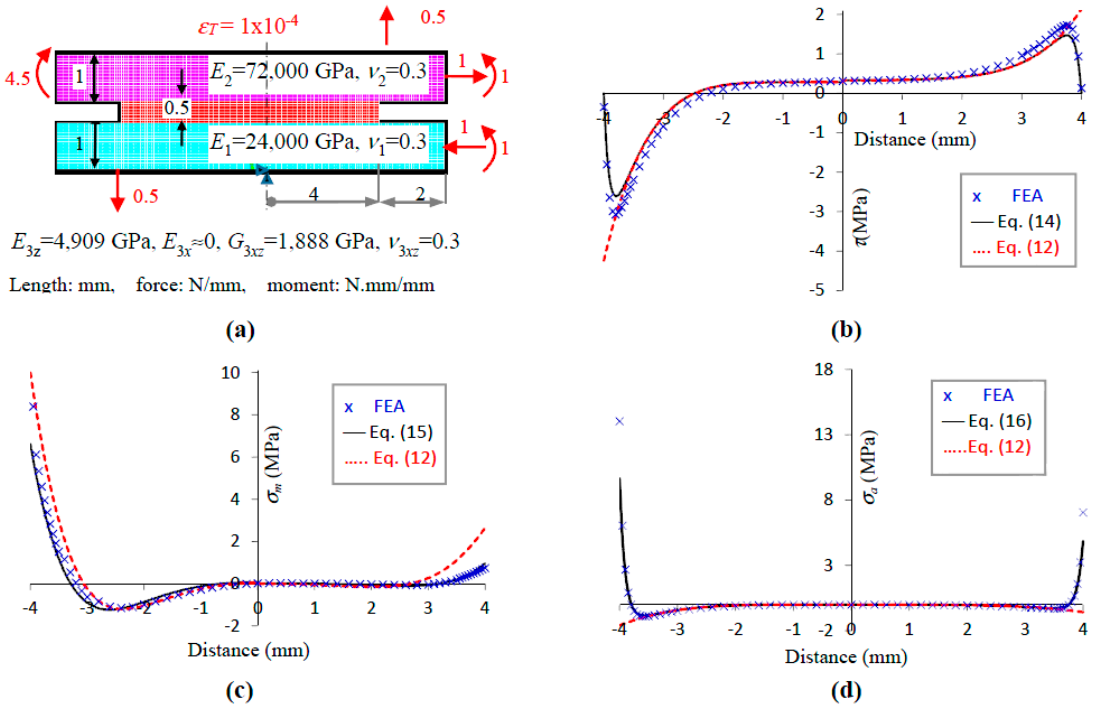

Figure 3. Numerical validation: (**a**) model; (**b**) $\tau(x)$; (**c**) $\sigma_m(x)$ and (**d**) $\sigma_a(x)$.

Table 1. Numerical validation: characteristics of the unbalanced structure.

Compliances		**Characteristic Parameters (mm^{-1})**				**Free Edge Parameters**	
κ_s	2.83×10^{-4}	α		1.08		ϕ	0.45
λ_x	4.31×10^{-4}	β		1.23		n	7.4
λ_z	1.21×10^{-4}	Coupling parameters (N^{-1})					
		μ_σ		1.67×10^{-4}		μ_τ	2.50×10^{-4}
Stress coefficients (N. mm^{-2})							
Domain	A_s	A_4	A_{p1}	A_{p2}	B_{1n}	B_{2n}	B_p
$-l \le x \le 0$	3.23	0.31	1.33	0.83	4.94	7.23	1.67
$0 \le x \le l$	1.53		0.3	0.1	0.35	0.98	0.61

κ_s, λ_z (N^{-1}.mm^3), λ_x (N^{-1}.mm).

4. Design Analysis

4.1. Balanced Structures

The shear stress in the adhesive for a balanced structure is given by Equation (5). For simplicity, we shall assume A_c » A_3, the maximum magnitude of shear stress is given by

$$\tau_{\max} \approx A_c = \frac{\varepsilon_T + \varepsilon_{Nl} + \varepsilon_{Ml}}{\sqrt{\lambda_x \kappa_s}} \tag{18}$$

For the same magnitude of the applied strains, the magnitude of shear stress may be reduced by increasing the x-compliance and the shear compliances of the bonded structure. We shall analyse two extreme cases; case I: the ratio $h_{\text{adhesive}}/h_{\text{adherend}}$ is significant such that the shear compliance of the structure is dominated by that of the adhesive; that is, $\kappa_s \approx h_3/G_3$, and case II: $h_{\text{adhesive}}/h_{\text{adherend}}$ is insignificantly small, such that the shear compliance of the structure is dominated by that of the adherends; that is, $\kappa_s \approx h_1/4G_1$. The product $\lambda_x \kappa_s$ for the two extreme cases (for plane stress) are given by:

$$\lambda_x \kappa_s = \begin{cases} \frac{2h_3/h_1}{E_1 G_3}(4 + 3h_3/h_1) & \text{Case I} \\ \frac{2}{E_1 G_1} & \text{Case II} \end{cases} \tag{19}$$

Thus, for Case I, the magnitude of shear stress in the adhesive may be reduced by reducing the elastic moduli of the adherends and the adhesive while increasing the thickness ratio of adhesive-to-adherend. For Case II, the magnitude of shear stress in the adhesive may be reduced by reducing the elastic modulus of the adherends.

The mean of the transverse stress in the adhesive, σ_m, for a balanced structure is given by Equation (9). The maximum magnitude of σ_m occurs at $x = l$ and is given by

$$\sigma_{m,\max} = B_{1c} = \frac{1}{2\alpha^2 \lambda_z}\left(\frac{\hat{Q}_{21l}}{\alpha} + \hat{M}_{21l}\right) \tag{20}$$

Noting that $2\alpha^2\lambda_z = \sqrt{\lambda_z \overline{D}}$, $\hat{Q}_{21l} = Q_{2l}/D_2 - Q_{1l}/D_1$, $\hat{M}_{21l} = M_{2l}/D_2 - M_{1l}/D_1$ and $D_1 = D_2$, for the same magnitude of the normalised edge forces, $(Q_{2l} - Q_{1l})/\alpha$, and the edge moments, M_{2l}-M_{1l}, the magnitude of $\sigma_{m,\max}$ may be reduced by increasing the product $\lambda_z \overline{D} {D_1}^2 = 2\lambda_z D_1$; that is, by increasing the z-compliance and the flexural stiffness of the structure. We shall analyse the same

two extreme cases described for shear stress : $\lambda_z \approx h_3/E_3$ for Case I and $\lambda_z \approx 13h_1/16E_1$ for Case II. The product $\lambda_z D_1$ for the two extreme cases (for plane stress) are given by:

$$\lambda_z D_1 = \begin{cases} \frac{{h_1}^3 h_3 E_1/E_3}{12} & \text{Case I} \\ \frac{13{h_1}^4}{192} & \text{Case II} \end{cases} \tag{21}$$

Thus, for Case I, the magnitude of $\sigma_{m,\max}$ may be reduced most effectively by increasing the thickness of the adherends and less effectively by increasing the thickness of the adhesive or the ratio of E_{adherend}-to-E_{adhesive}. For Case II, the magnitude of $\sigma_{m,\max}$ may be reduced very effectively by increasing the thickness of the adherends.

The amplitude of the transverse stress in the adhesive, σ_a, for a balanced structure is given by Equation (11), which however ought to be modified to include the free-edge condition:

$$\sigma_a(x) = -\frac{h_3}{2}\left\{\left(1 - e^{n\beta(x-l)}\right)\beta A_c e^{\beta(x-l)} - n\beta e^{n\beta(x-l)}\left[A_c e^{\beta(x-l)} + A_3\right]\right\} \tag{22}$$

The maximum magnitude of σ_m occurs at $x = l$. For simplicity, we shall assume $A_c \gg A_3$; the maximum magnitude of σ_a, after substituting the exponential factor n with Equation B(2) is given approximately by

$$\sigma_{a,\max} \approx \frac{n\beta h_3 A_c}{2} \approx \frac{0.72 A_c}{\varphi^{1.4}(\beta h_3)^{0.4}} \approx \frac{0.72}{\varphi^{1.4}} \frac{\varepsilon_T + \varepsilon_{Nl} + \varepsilon_{Ml}}{\sqrt[4]{{\lambda_x}^3 \kappa_s {h_3}^2}} \tag{23}$$

Assuming ϕ to be a constant, then for the same magnitudes of the applied strains, the magnitude of $\sigma_{a,\max}$ may be reduced by increasing the product ${\lambda_x}^3 \kappa_s {h_3}^2$, which for the two extreme cases: $\kappa_s \approx h_3/G_3$ for Case I and $\kappa_s \approx h_1/4G_1$ for Case II - are given by (for plane stress)

$${\lambda_x}^3 \kappa_s {h_3}^2 = \begin{cases} \frac{8(h_3/h_1)^3(4+3h_3/h_1)^3}{{E_1}^3 G_3} & \text{Case I} \\ \frac{128(h_3/h_1)^2}{{E_1}^3 G_1} & \text{Case II} \end{cases} \tag{24}$$

Thus, for Case I, the magnitude of $\sigma_{a,\max}$ may be reduced most effectively by reducing the elastic modulus of the adherends or by increasing the thickness ratio of adhesive-to-adherend and less effectively by reducing the elastic modulus of the adhesive. For Case II, the magnitude of $\sigma_{m,\max}$ may be reduced most effectively by reducing the elastic modulus of the adherends and less effectively by increasing the thickness ratio of adhesive-to-adherend.

It is clear from the above that the design guidelines do not concurrently minimise $\tau_{\max}$, $\sigma_{a,\max}$, and $\sigma_{m,\max}$. In other words, the design guidelines for minimizing the magnitudes of $\tau_{\max}$, $\sigma_{a,\max}$, and $\sigma_{m,\max}$ are contradictory. We shall examine the relative magnitudes of these components of stress. Equation (25) presents the ratio of $\sigma_{a,\max}/\tau_{\max}$. It is noted that the magnitude of $\sigma_{a,\max}$ is almost always larger than that of $\tau_{\max}$. This, together with the fact that the peeling strength of a bonded joint is generally weaker than its shear strength, suggests that it is more important to minimise the magnitudes of $\sigma_{a,\max}$ and $\sigma_{m,\max}$ than the magnitude of $\tau_{\max}$.

$$\begin{aligned} \tfrac{\sigma_{a,\max}}{\tau_{\max}} &= \tfrac{n\beta h_3}{2} \approx \tfrac{0.72}{\varphi^{1.4}(\beta h_3)^{0.4}} \approx \tfrac{2}{(\beta h_3)^{0.4}} \text{ assuming } \varphi = 0.5 \\ &\approx 2\left[\tfrac{E_1 h_1}{2G_3 h_3 (4+3h_3/h_1)}\right]^{0.2} \text{ for Case I} \\ &\approx 3 \text{ to } 4 \text{ for } E_1 h_1 / G_3 h_3 \text{ between 60 to 250} \end{aligned} \tag{25}$$

Equation (26) presents the ratio of $\sigma_{a,\max}/\sigma_{m,\max}$. Noting that $\sigma_{m,\max} \approx 0$ for adherends experiencing only thermal strain and/or stretching strain, $\sigma_{a,\max}$ is much larger than $\sigma_{m,\max}$ for

these cases. Noting that $\sigma_{a,\max} \approx 0$ for adherends experiencing only edge shear forces, Q_{il}, $\sigma_{a,\max}$ is much smaller than $\sigma_{m,\max}$ for this case. Thus, $\sigma_{a,\max}$ may be larger or smaller than $\sigma_{m,\max}$ for a general loading condition. For the case of single lap-joints (SLJ) that are dominated by stretching and bending through a single adherend, i.e., $\varepsilon_T = 0$, $\hat{Q}_{21l} \approx 0$, $\kappa_{1l} = 0$, while N_{2l} and M_{2l} are positive, $\sigma_{a,\max}$ is almost always larger than $\sigma_{m,\max}$. It is therefore advisable to give more weight to the design guidelines that minimize the magnitude of $\sigma_{a,\max}$.

$$\begin{aligned} \frac{\sigma_{a,\max}}{\sigma_{m,\max}} &= \frac{n\beta h_3}{2}\sqrt{\frac{\lambda_z\overline{D}}{\lambda_x\kappa_s}}\frac{\varepsilon_T+\varepsilon_{Nl}+\varepsilon_{Ml}}{\hat{Q}_{21l}/\alpha+\hat{M}_{21l}} \\ &\approx \frac{n\beta h_3}{4}\sqrt{\frac{6}{(4+3h_3/h_1)(1+\nu)}}\left(\frac{N_{2l}h_1}{6M_{2l}}+1+h_3/h_1\right) > 1 \text{ for SLJ and Case I} \end{aligned} \tag{26}$$

4.2. Unbalanced Structures

In light of the coupling of τ(x) and $\sigma_m(x)$ for the unbalanced structures, it is improbable to find a universal guideline for the optimum design of unbalanced structures that can be expressed in the simple forms of Equations (19), (21) and (24).

The shear stress in the adhesive of an unbalanced structure is given by Equation (14). For simplicity, we shall assume A_s » A_4 while also ignoring the decay function, $1 - e^{n\beta(x-l)}$, the maximum magnitude of shear stress is then given by

$$\begin{aligned} \tau_{\max} &\approx A_s + A_{p1} = A_c - \frac{\alpha}{\beta}\left(A_{p1}+A_{p2}\right) + A_{p1} \\ &= \frac{\varepsilon_T+\varepsilon_{Nl}+\varepsilon_{Ml}}{\sqrt{\lambda_x\kappa_s}} + \frac{\mu_\sigma\left[\left(2\alpha^3-2\alpha^2\beta+\alpha\beta^2\right)\hat{Q}_{21l}/\alpha+\left(-4\alpha^4/\beta+4\alpha^3-2\alpha^2\beta\right)\hat{M}_{21l}\right]}{4\alpha^4\left(4\alpha^4+\beta^4\right)\lambda_z\kappa_s} \end{aligned} \tag{27}$$

The magnitude of A_c may be reduced by increasing the x-compliance and the shear compliance of the structure. Equation (27) suggests that the magnitude of the particular solution may be reduced by increasing the product $\left(4\alpha^4+\beta^4\right)\lambda_z\kappa_s$, which implies increasing the x-compliance and the flexural compliance of the structure. While increasing the x-compliance of the structure would reduce the magnitudes of both the complimentary and particular solutions, this does not imply that it will always lead to reduced magnitude of the $\tau_{\max}$ of the unbalanced structure. This is because ε_T, ε_{Nl}, ε_{Ml}, $\hat{Q}_{21l}$, $\hat{M}_{21l}$ and μ_σ could be either positive or negative and hence the particular solution may not act in the same direction as the complementary solution. Nevertheless, increasing the x-compliance of the structure is more likely than not to reduce the $\tau_{\max}$ of an unbalanced structure. In the same breath, it should be noted that the magnitude of $\tau_{\max}$ in an unbalanced structure may not always be larger than that in a balanced structure assuming both structures have identical characteristic parameters.

The mean of the transverse stress in the adhesive, σ_m, for an unbalanced structure is given by Equation (15). For the reason of simplicity, we shall ignore those terms associated with the decay function. The maximum magnitude of σ_m occurs at $x = l$ and is given by

$$\begin{aligned} \sigma_{m,\max} &\approx B_1 + B_p = B_{1c} + \left(\frac{\beta^3}{2\alpha^3} - \frac{\beta^2}{2\alpha^2} + 1\right)B_p \\ &= \frac{1}{\sqrt{\overline{D}\lambda_z}}\left[\frac{\hat{Q}_{21l}}{\alpha} + \hat{M}_{21l} + \frac{\mu_\tau\left(\beta^4/\alpha-\beta^3+2\alpha^2\beta\right)}{4\alpha^4+\beta^4}\frac{\varepsilon_T+\varepsilon_{Nl}+\varepsilon_{Ml}}{\beta\kappa_s}\right] \end{aligned} \tag{28}$$

Noting that $\hat{Q}_{21l} = Q_{2l}/D_2 - Q_{1l}/D_1$ and $\hat{M}_{21l} = M_{2l}/D_2 - M_{1l}/D_1$, for the same magnitudes of Q_{il} and M_{il}, the magnitude of B_1 may be reduced by increasing the z-compliance while reducing the flexural compliance of the structures. Equation (28) suggests that the magnitude of the particular solution may be reduced by increasing the magnitudes of the characteristic parameter, α, which implies increasing the flexural compliance of the structure while reducing the z-compliance of the structure. This is in reverse to the trend for B_p.

The amplitude of the transverse stress in the adhesive, σ_a, for an unbalanced structure is given by Equation (16). Assuming $A_s \gg A_4$, the maximum magnitude of σ_a is given by:

$$\sigma_{a,\max} \approx \frac{n\beta h_3 \left(A_s + A_{p1}\right)}{2} \approx \frac{n\beta h_3}{2}\tau_{\max} \approx \frac{0.72}{\varphi^{1.4}(\beta h_3)^{0.4}}\tau_{\max} \tag{29}$$

which again suggests that the magnitude of $\sigma_{a,\max}$ is likely to be reduced by increasing the x-compliance of the structure.

It has been argued in the previous section that the magnitude of $\sigma_{a,\max}$ is almost always larger than that of $\tau_{\max}$ for balanced structures. Comparing Equations (23) and (29), it is reasonably safe to suggest that this will also be the case for unbalanced structures. It has been established in the previous section that the ratio of $\sigma_{a,\max}$ to $\sigma_{m,\max}$ for balanced SLJ is larger than unity. If the ratio for the particular solutions is also larger than unity then one can safely assume that the ratio of $\sigma_{a,\max}$ to $\sigma_{m,\max}$ for unbalanced SLJ is also larger than unity. The ratio for the particular solutions is given by

$$\frac{\sigma_{a,\max}}{\sigma_{m,\max}} \approx \frac{n\beta h_3}{2}\frac{\mu_\sigma\left(-2\alpha^2/\beta + 2\alpha - \beta\right)\kappa_{2l}}{\mu_\tau(\beta^3/\alpha - \beta^2 + 2\alpha^2)\frac{\varepsilon_{Nl}+\varepsilon_{Ml}}{\sqrt{\lambda_x\kappa_s}}} \tag{30}$$

which is not necessary larger than unity. Thus, $\sigma_{a,\max}$ is only conditionally larger than $\sigma_{m,\max}$ for unbalanced SLJ.

Given the loadings and the design space, the optimum designs of unbalanced structure that gives rise to a minimum $\tau_{\max}$, a minimum $\sigma_{m,\max}$, and a minimum $\sigma_{a,\max}$, respectively, can be readily established using Equations (27)–(29).

5. Conclusions

Strength-of-material solutions for the shear stress, τ, the mean, σ_m, and amplitude, σ_a, of the peeling stress in both balanced and unbalanced structures have been derived and used for design analysis. Design guidelines for balanced structures have been established. The magnitude of $\sigma_{a,\max}$ for balanced structures is almost always larger than that of $\tau_{\max}$ and the magnitude of $\sigma_{a,\max}$ for balanced single-lap-joints is also almost always larger than $\sigma_{m,\max}$. The magnitude of $\sigma_{a,\max}$ for balanced structures may be reduced most effectively by reducing the elastic modulus of the adherends or by increasing the thickness ratio of adhesive-to-adherend and less effectively by reducing the elastic modulus of the adhesive. The simple expressions of $\tau_{\max}$, $\sigma_{m,\max}$ and $\sigma_{a,\max}$ established in this manuscript for the unbalanced structures will help practicing engineers find the optimum design within the given design space.

Acknowledgments: The financial support from Ministry of Science and Technology, China for the key program contract No. 2017YFB040600.

Author Contributions: Ee-Hua Wong and Johan Liu established the theories; Ee-Hua Wong wrote the paper.

Conflicts of Interest: The authors declare no conflict of interest.

Nomenclatures

Subscript #$_i$	Subscript #1 and #2 are adherends and #3 is adhesive.
D_i, E_i, G_i, h_i	Flexural rigidity, elastic modulus, shear modulus, thickness of member #i.
$\overline{D}$	Flexural compliance of the bonded structure.
$M_{\pm il}$, $N_{\pm il}$, $Q_{\pm il}$	Moment, sectional stretching force, sectional shear force applied on adherend #i at $x = \pm l$.
l	Half-length of the bonded structure.
α, β	Characteristic parameters of a bonded structure in peeling, shearing.
α_i	Coefficient of thermal expansion of adherend #i.
ε_T, $\varepsilon_{\pm Nl}$, $\varepsilon_{\pm Ml}$	Differential strain between adherends #2 and #1 at $x = \pm l$ due to temperature and edge stretching; effective bending strain due to edge bending at $x = \pm l$.

$\kappa_{\pm il}$	Edge curvature of adherend #*i* at $x = \pm l$.
κ_{si}, κ_s	Shear compliance of member #*i*, of the bonded structure between the centroid planes of adherends #1 and #2.
λ_{xi}, λ_x	x-compliance of adherend #*i*, of the bonded structure.
$\lambda_{x\theta}$	Additional x-compliance of the bonded structure attributed to its flexural deformation.
λ_{zi}, λ_z	z-compliance of member #*i*, of the bonded structure between the centroid planes of adherends #1 and #2.
θ_i	Rotation of the centroid axis of adherend #*i* (due to bending).
$\sigma_m(x)$, $\sigma_a(x)$	Mean, amplitude of variation, of transverse stress along the thickness of the adhesive (or between the bonded interfaces).
$\sigma_p(x)$	Peeling stress along the bonded interfaces.
$\tau(x)$	Shear stress within the adhesive (and along the interfaces).
ΔT	Temperature change.

Basic formulas

$4\alpha^4 = \frac{\overline{D}}{4\lambda_z}$; $\beta^2 = \frac{\lambda_x}{\kappa_s}$.

$D_i = \frac{E_i h_i^3}{12}$(plane stress); $\overline{D} = \frac{1}{D_1} + \frac{1}{D_2}$.

$\kappa_s = \kappa_{s1} + \kappa_{s2} + \kappa_{s3}$

$\kappa_{si} \approx \frac{h_i}{8G_i}, i = 1, 2; \kappa_{s3} = \frac{h_3}{G_3}$

$\lambda_x = \lambda_{x1} + \lambda_{x2} + \lambda_{x\theta}$

$\lambda_{xi} = \frac{1}{E_i h_i}$, $i = 1, 2$; $\lambda_{x\theta} = \frac{1}{4}\left[\frac{h_1(h_1+h_3)}{D_1} + \frac{h_2(h_2+h_3)}{D_2}\right]$

$\lambda_z = \lambda_{z1} + \lambda_{z2} + \lambda_{z3}$

$\lambda_{zi} \approx \frac{13}{32}\frac{h_i}{E_i}$, $i = 1, 2; \lambda_{z3} = \frac{h_3}{E_3}$

$\mu_\sigma = \frac{1}{2}\left(\frac{h_2}{D_2} - \frac{h_1}{D_1}\right), \mu_\tau = \frac{1}{2}\left(\frac{h_2+h_3}{D_2} - \frac{h_1+h_3}{D_1}\right)$

Appendix A. Fundamental Equations

Refers to Figure 2, assuming the traction N_i passes through the centroid plane of adherend #1, the equilibriums of the differential elements gives

$$\begin{aligned} dN_i &= \mp\tau dx \\ dQ_i &= (\mp\sigma_m + \sigma_a)dx \\ dQ_3 &= -2\sigma_a dx \quad i = 1,\ 2 \\ dM_i &= \left(\frac{\tau h_i}{2} - Q_i\right)dx \end{aligned} \tag{A1}$$

where the upper and the lower signs in "$\mp$" refers to adherend #1 and #2, respectively. The x-directional traction-stretching relation of the centroid plane of adherend #*i* is given by:

$$\frac{du_i}{dx} - \alpha_i \Delta T = N_i \lambda_{xi} \tag{A2}$$

The moment-rotation relation of the centroid plane of adherend #*i* is assumed to obey simple beam:

$$\frac{d^3 w_i}{dx^3} = \frac{d^2\theta_i}{dx^2} = \frac{1}{D_i}\frac{dM_i}{dx} = \frac{1}{D_i}\left(\frac{h_i\tau}{2} - Q_i\right) \tag{A3}$$

The differential displacement of the centroid planes of adherend #1 and #2 in the u-direction and in the z-direction are given by:

$$\begin{aligned} u_2 - u_1 &= \kappa_s \tau - \frac{h_1\theta_1 + h_2\theta_2}{2} \\ w_2 - w_1 &= \lambda_z \sigma_m \end{aligned} \tag{A4}$$

where θ_i is the rotation of the neutral axis of member #*i*. Differentiating Equation (A2) twice with respect to x followed by taking the difference between adherend #2 and #1, and equating with the third differential of the first equation of (A4) gives the differential equation:

$$\frac{d^3\tau}{dx^3} - \beta^2\frac{d\tau}{dx} = -\frac{\mu_\sigma}{k_s}\sigma_m \tag{A5}$$

Differentiating Equation (A3) with respect to x followed by taking the difference between adherends #2 and #1, and equating with the fourth differential of the second equation of (A4) gives the differential equation

$$\frac{d^4\sigma^m}{dx^4} + 4\alpha^4\sigma^m = \frac{\mu_\tau}{\lambda_z}\frac{d\tau}{dx} \tag{A6}$$

The parameters and the coefficients are given by

$$\begin{aligned} &\beta^2 = \tfrac{\lambda_x}{\kappa_s},\ 4\alpha^4 = \tfrac{\overline{D}}{\lambda_z} \\ &\lambda_x = \lambda_{x1} + \lambda_{x2} + \sum_{i=1}^{2} \tfrac{h_i(h_i+h_3)}{4D_i} \\ &\kappa_s = \sum_{i=1}^{3} \kappa_{si},\ \lambda_z = \sum_{i=1}^{3} \lambda_{zi},\ D = \sum_{i=1}^{2} \tfrac{D_i}{1} \\ &\mu_\sigma = \tfrac{1}{2}\left(\tfrac{h_2}{D_2} - \tfrac{h_1}{D_1}\right),\ \mu_\tau = \tfrac{1}{2}\left(\tfrac{h_2+h_3}{D_2} - \tfrac{h_1+h_3}{D_1}\right) \end{aligned} \tag{A7}$$

Appendix B. Imposing Free-Edge Condition

The free-edge condition, $\tau(l) = 0$, can be artificially imposed by multiplying the expression of the shear stress, Equation (12), with a decay function $1-e^{n\beta(x-1)}$, wherein n is a positive real number with a magnitude significantly larger than unity such that the decay function diminishes rapidly from the free edge towards $x = 0$. Assuming (i) $\tau_c(x) \approx A_c e^{\beta(x-l)}(1-e^{n\beta(x-l)})$ and (ii) the stationary point of $\tau(x)$ occurs at a distance φh_3 from the free edge, where φ is assumed to be a constant, the magnitude of n may be evaluated approximately by differentiating $\tau_c(x)$ with respect to x followed by equating the stationary point with $l-\varphi h_3$. This yields:

$$n = e^{n\varphi\beta h_3} - 1 \approx 1.43(\varphi\beta h_3)^{-1.40} \tag{A8}$$

which for ease of engineering manipulation may be approximated as

$$n \approx 1.43(\varphi\beta h_3)^{-1.40} \tag{A9}$$

The "constant" ϕ is approximately 0.5 but has been established through collocating with the finite element analysis as:

$$\varphi \approx 0.407(\beta {h_3}^{0.88})^{-0.26} \tag{A10}$$

for $0.018 \leq \beta h_3 \leq 1.73$.

References

1. Volkersen, Q. Die NietKraftverteilung in zugbeanspruchten Nietverbindungen mit Konstanten Laschenquerschnitten. *Luftfahrtforschung* **1938**, *15*, 41–47.
2. Goland, M.; Reissner, E. Stresses in cemented joints. *ASME J. Appl. Mech.* **1944**, *11*, A17–A27.
3. Tsai, M.Y.; Oplinger, D.W.; Morton, J. Improved theoretical solutions for adhesive lap joints. *Int. J. Solids Struct.* **1998**, *35*, 1163–1185. [CrossRef]
4. Suhir, E. Stresses in bi-metal thermostats. *ASME J. Appl. Mech.* **1986**, *53*, 657–660. [CrossRef]
5. Suhir, E. Interfacial stresses in bimetal thermostats. *ASME J. Appl. Mech.* **1989**, *56*, 595–600. [CrossRef]
6. Timoshenko, S.P.; Goodier, J.N. *Theory of Electricity*, 3rd ed.; McGraw-Hill: New York, NY, USA, 1970.
7. Chen, W.T.; Nelson, C.W. Thermal Stress in Bonded Joint. *IBM J. Res. Dev.* **1979**, *23*, 179–188. [CrossRef]
8. Delale, F.; Erdogan, F.; Aydinoglu, M.N. Stresses in adhesively bonded joints: A closed-form solution. *J. Compos. Mater.* **1981**, *15*, 249–271. [CrossRef]
9. Bigwood, D.A.; Crocombe, A.D. Elastic analysis and engineering design formulae for bonded joints. *Int. J. Adhes. Adhes.* **1989**, *9*, 229–242. [CrossRef]
10. Zou, G.P.; Shahin, K.; Taheri, F. An analytical solution for the analysis of symmetric composite adhesively bonded joints. *Compos. Struct.* **2004**, *65*, 499–510. [CrossRef]
11. Liu, Z.; Huang, Y.; Yin, Z.; Bennati, S.; Valvo, P.S. A general solution for the two-dimensional stress analysis of balanced and unbalanced adhesively bonded joints. *Int. J. Adhes. Adhes.* **2014**, *54*, 112–123. [CrossRef]

12. Cabello, M.; Zurbitu, J.; Renart, J.; Turon, A.; Martínez, F. A general analytical model based on elastic foundation beam theory for adhesively bonded DCB joints either with flexible or rigid adhesives. *Int. J. Solids Struct.* **2016**, *94*, 21–34. [CrossRef]
13. Ojalvo, I.U.; Eidinoff, H.L. Bond thickness effects upon stresses in single-lap adhesive joints. *AIAA J.* **1978**, *16*, 204–211. [CrossRef]
14. Wang, J.; Zhang, C. Three-parameters, elastic foundation model for analysis of adhesively bonded joints. *Int. J. Solids Struct.* **2009**, *29*, 495–502. [CrossRef]
15. Wong, E.H. The mechanics of bondline thickness in balanced sandwich structures. *Int. J. Adhes. Adhes.* **2017**, *78*, 4–12. [CrossRef]
16. Zhao, B.; Lu, Z.-H.; Lu, Y.-N. Closed-form solutions for elastic stress–strain analysis in unbalanced adhesive single-lap joints considering adherend deformations and bond thickness. *Int. J. Solids Struct.* **2011**, *31*, 434–445. [CrossRef]
17. Zhang, Z.-W.; Li, Y.-S.; Liu, R. An analytical model of stresses in adhesive bonded interface between steel and bamboo plywood. *Int. J. Solids Struct.* **2015**, *52*, 103–113. [CrossRef]
18. Allman, D. A theory for elastic stresses adhesive bonded lap joints. *Q. J. Mech. Appl. Math.* **1977**, *30*, 10–15. [CrossRef]
19. Chen, D.; Cheng, S. An analysis of adhesive-bonded single-lap joints. *ASME J. Appl. Mech.* **1983**, *50*, 109–115. [CrossRef]
20. Yin, W.-L. Thermal stresses and free-edge effects in laminated beams: A variational approach using stress fFunctions. *ASME J. Electron. Packag.* **1991**, *113*, 68–75. [CrossRef]
21. Adams, R.D.; Mallick, V. A method for the stress analysis of lap joints. *J. Adhes.* **1992**, *38*, 199–217. [CrossRef]
22. Wu, X.F.; Zhao, Y. Stress-function variational method for interfacial stress analysis of adhesively bonded joints. *Int. J. Solids Struct.* **2013**, *50*, 4305–4319. [CrossRef]
23. Wong, E.H. Design analysis of sandwiched structures experiencing differential thermal expansion and differential free-edge stretching. *Int. J. Adhes. Adhes.* **2016**, *65*, 19–27. [CrossRef]